Identification of Cancer Stem Cells in Ewing's Sarcoma

Mario-Luca Suvà,[1] Nicolò Riggi,[1] Jean-Christophe Stehle,[1] Karine Baumer,[1] Stéphane Tercier,[2] Jean-Marc Joseph,[2] Domizio Suvà,[3] Virginie Clément,[4] Paolo Provero,[5] Luisa Cironi,[1] Maria-Chiara Osterheld,[1] Louis Guillou,[1] and Ivan Stamenkovic[1]

[1]Division of Experimental Pathology and Division of Clinical Pathology, Institute of Pathology and [2]Department of Pediatric Surgery, University of Lausanne, Lausanne, Switzerland; Departments of [3]Orthopedics and [4]Neurosurgery, University of Geneva, Geneva, Switzerland; and [5]Department of Genetics, Biology, and Biochemistry, University of Turin, Turin, Italy

Abstract

Cancer stem cells that display tumor-initiating properties have recently been identified in several distinct types of malignancies, holding promise for more effective therapeutic strategies. However, evidence of such cells in sarcomas, which include some of the most aggressive and therapy-resistant tumors, has not been shown to date. Here, we identify and characterize cancer stem cells in Ewing's sarcoma family tumors (ESFT), a highly aggressive pediatric malignancy believed to be of mesenchymal stem cell (MSC) origin. Using magnetic bead cell separation of primary ESFT, we have isolated a subpopulation of CD133+ tumor cells that display the capacity to initiate and sustain tumor growth through serial transplantation in nonobese diabetic/severe combined immunodeficiency mice, re-establishing at each *in vivo* passage the parental tumor phenotype and hierarchical cell organization. Consistent with the plasticity of MSCs, *in vitro* differentiation assays showed that the CD133+ cell population retained the ability to differentiate along adipogenic, osteogenic, and chondrogenic lineages. Quantitative real-time PCR analysis of genes implicated in stem cell maintenance revealed that CD133+ ESFT cells express significantly higher levels of *OCT4* and *NANOG* than their CD133− counterparts. Taken together, our observations provide the first identification of ESFT cancer stem cells and demonstration of their MSC properties, a critical step towards a better biological understanding and rational therapeutic targeting of these tumors. [Cancer Res 2009;69(5):1776–81]

Introduction

Ewing's sarcoma family tumors (ESFT) are the second most frequent malignant bone tumors in adolescents and young adults. Despite current multimodal therapy, they are associated with poor prognosis, with a survival rate of <50% at 5 years and <25% when metastasis has occurred. ESFTs typically harbor a specific chromosomal translocation that results in the fusion of the 5′ portion of the *EWS* gene to the 3′ portion of one of at least five genes that encode ETS family transcription factors, including *FLI1, ERG, ETV1, ETV4*, and *FEV* (1, 2). In 85% of cases, ESFT are associated with the t(11;22)(q24;q12) translocation (1), which generates the *EWS-FLI-1* fusion gene believed to play a central role in ESFT pathogenesis. Recent evidence suggests that ESFT arise from EWS-FLI-1–transformed mesenchymal stem cells (MSC; refs. 3–5) but most of our current understanding of ESFT biology is still based on studies using established cell lines, which may only partially reflect the cellular hierarchy that governs primary tumor growth and differentiation.

The cancer stem cell (CSC) hypothesis holds that cells composing a tumor are hierarchically organized with respect to their potential to initiate and sustain tumor growth (6). Only a rare subset of tumor cells, defined as CSCs, have the capacity to form tumors in serial xenotransplantation assays, and the ability to re-establish, at each *in vivo* passage, the hierarchical cell organization and heterogeneity of the parental tumor. Recently, CSC have been identified in leukemias (7), gliomas (8, 9), melanomas (10), and different types of carcinomas (11–13), providing a biological basis for the design of rational targeted therapy. Here, using primary, surgically removed tumor samples, we identify for the first time a population of ESFT cells expressing CD133 that fulfil the *in vivo* criteria of CSC and display *in vitro* MSC's plasticity.

Materials and Methods

Fresh tumor dissociation, magnetic cell sorting, and fluorescence-activated cell sorting analysis. Tumor samples of ESFTs from three patients undergoing surgical biopsies were obtained directly after surgical removal in accordance with local legislation. Tumor samples were mechanically dissociated, digested in collagenase II/IV (Sigma), and incubated in a shaking water bath for 2 h at 37°C. Preseparation filters (Miltenyi) were used to remove clumps and erythrolysis was performed in hypotonic solution (0.2% NaCl, followed by 1.2% NaCl to stop lysis). Cell viability was assessed by trypan blue staining, and whenever viability was <90%, samples were purified with the dead cell removal kit (Miltenyi). Single cell suspensions were then incubated with CD133 microbeads (Miltenyi) and separated using an autoMACS device (Miltenyi), according to the manufacturer's instructions. Prior to and following separation, samples were analyzed by fluorescence-activated cell sorting (FACS) using CD133/2 phycoerythrin (293C3, 1/10) antibody (Miltenyi) and isotype control mouse IgG_{2b} phycoerythrin (1/10; Miltenyi) in a FACScalibur apparatus (Becton Dickinson).

Nonobese diabetic/severe combined immunodeficiency xenotransplantation. Twenty-four hours prior to transplantation, 8- to 10-week-old nonobese diabetic (NOD)/severe combined immunodeficiency (SCID) mice were sublethally irradiated (3.4 Gy). Tumor samples were xenotransplanted into the subcapsular compartment of the left kidney of anaesthetized NOD/SCID mice using a 1:1 mixture with Matrigel (BD Bioscience). Prior to xenotransplantation, the viability of the samples was verified by a trypan blue exclusion assay. For small numbers of injected cells, >75% viability was needed for tumors to develop. Experimental procedures involving mice were approved by the Etat de Vaud, Service Vétérinaire, authorization no. VD1477.2.

Note: Supplementary data for this article are available at Cancer Research Online (http://cancerres.aacrjournals.org/).

M-L. Suvà and N. Riggi contributed equally to this work.

Requests for reprints: Ivan Stamenkovic, University of Lausanne, 25 Rue du Bugnon, Lausanne CH-1011, Switzerland. Phone: 41-21-314-7136; Fax: 41-21-314-7110; E-mail: Ivan.Stamenkovic@chuv.ch.

doi:10.1158/0008-5472.CAN-08-2242

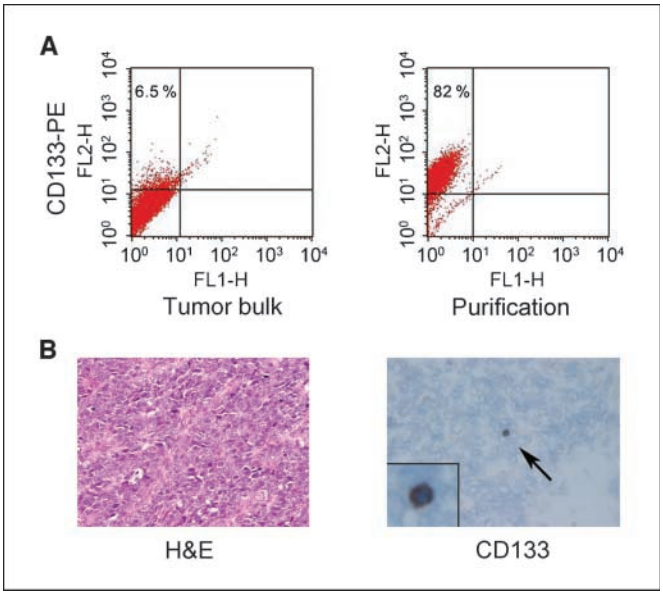

Figure 1. Identification of CD133+ cells in primary ESFTs. *A,* CD133 phycoerythrin (*PE*) FACS analysis of ESFT-derived single cell suspensions, before and after CD133 magnetic bead purification, showing the presence, and subsequent enrichment, of a CD133+ subpopulation. *B,* H&E staining and anti-CD133 immunohistochemical analysis of primary ESFT frozen sections showing the typical ESFT small round cell morphology, and allowing the identification of rare CD133+ cells in the tumor. Magnification, ×200 (*inset,* ×600).

Cell culture and differentiation. Freshly dissociated tumor samples were cultivated as spheres in DMEM-F12 (Life Technologies), supplemented with 20% knockout serum replacement (Life Technologies 10828), 10 ng/mL of recombinant human epidermal growth factor (Invitrogen), 10 ng/mL of recombinant human basic fibroblast growth factor (Invitrogen), and 1% penicillin/streptomycin (Life Technologies). For differentiation assays, grown spheres were expanded as adherent cultures in MSC medium for 1 week [IMDM (Life Technologies), 10% FCS and 10 ng/μL platelet-derived growth factor BB (PeProtechEC)] and then tested for multilineage differentiation as previously described (14). Briefly, for chondrogenic differentiation, 300,000 cells were centrifuged in a 15 mL polypropylene conical tube and incubated in DMEM (Life Technologies 31966) supplemented with 10^{-7} mol/L dexamethasone (Sigma D1756), 1% insulin, transferrin, and selenium, 100 μmol/L L-ascorbic acid 2-phosphate (Sigma A8960), and 10 ng/mL of transforming growth factor-β1 (R&D Systems). Cells were cultured for 4 weeks with medium replacement twice per week. For adipogenic differentiation, cells were seeded at 30,000 cells/well in a 24-well tissue culture plate and grown in DMEM hi-glucose (Life Technologies 31966) with 10% FCS until confluent. Cells were maintained at confluence for 5 days and then incubated in induction medium, consisting of DMEM low-glucose (Life Technologies 21885), 10% FCS, 10 μg/mL insulin (Sigma I9278), 10^{-6} mol/L dexamethasone, 5×10^{-4} mol/L 3-isobutyl-1-methylxanthine (Sigma I5879), and 10^{-4} mol/L indomethacine (Sigma I7378). After 48 h, this medium was washed out and replaced by maintenance medium consisting of DMEM hi-glucose (Life Technologies 31966), 10% horse serum, and 10^{-6} mol/L dexamethasone for 4 days. This induction-maintenance cycle was repeated thrice and cells were then cultured in maintenance medium until adipocytes became visible. For osteogenic differentiation, 50,000 cells were seeded in a 12-well tissue culture plate in MSC medium. Twenty-four hours later, medium was washed out and replaced by differentiation medium consisting of DMEM low-glucose supplemented with 10% FCS, 10 mmol/L B-glycerophosphate (Sigma, G9891), 10^{-7} mol/L dexamethasone, and 100 μmol/L L-ascorbic acid 2-phosphate (Sigma A8960). Cells were maintained in differentiation medium for 10 to 14 days, with fresh medium replacement twice per week.

Clonogenic assay. For clonogenic assays, three bulk tumor samples were disaggregated and the resulting cells were sorted for CD133 expression using CD133 microbeads (Miltenyi) and an autoMACS device (Miltenyi). To further improve the purity of the CD133− fraction, a second sorting step was performed, adding fresh CD133 microbeads to the CD133− cell fraction and running a depletion program on the autoMACS. The initial CD133+ and

Table 1. ESFT-derived CD133+ cells display cancer-initiating properties

Samples	No. of cells injected	Fraction of injected NOD/SCID mice bearing tumors after 3 mo						
		First transplant			Second transplant		Third transplant	
		Tumor bulk	CD133+	CD133−	CD133+	CD133−	CD133+	CD133−
ESFT 1	50,000	4/6	6/6	0/6	6/6	0/6	6/6	0/6
	10,000	0/6	6/6	0/6	4/6	0/6	6/6	0/6
	2,500	0/6	3/6	0/6	2/6	0/6	3/6	0/6
	500	0/6	0/6	0/6	0/6	0/6	0/6	0/6
ESFT 2	50,000	2/6	6/6	0/6	6/6	0/6	6/6	0/6
	10,000	0/6	5/6	0/6	6/6	0/6	5/6	0/6
	2,500	0/6	1/6	0/6	4/6	0/6	2/6	0/6
	500	0/6	0/6	0/6	0/6	0/6	0/6	0/6
ESFT 3	50,000	3/6	6/6	0/6	6/6	0/6	6/6	0/6
	10,000	0/6	5/6	0/6	5/6	0/6	6/6	0/6
	2,500	0/6	2/6	0/6	2/6	0/6	3/6	0/6
	500	0/6	0/6	0/6	0/6	0/6	0/6	0/6

NOTE: *In vivo* tumorigenicity experiments were performed using CD133+ and CD133− cells derived from three different ESFT samples. For each tumor sample, six sublethally irradiated NOD/SCID mice were injected with CD133+ or CD133− cells in decreasing numbers. Tumors were observed to arise exclusively from the CD133+ fractions and were subsequently used for serial transplantation of the corresponding CD133+ and CD133− purified fractions. The table shows the number of tumor-bearing mice 12 wk following injection of CD133+ and CD133− cells, for each injected cell number and transplantation passage.

the depleted CD133− fractions were plated as single cells in 10 × 96-well plates and cultivated for 30 days in sphere medium with fresh medium added weekly to renew the growth factor supply.

Immunohistochemistry. Frozen primary Ewing's sarcoma samples were incubated with CD133/2 antibody (Miltenyi, clone 293C3) at a 1:50 dilution, overnight. Paraffin-embedded sections of primary Ewing's sarcoma, and serial mouse transplants were incubated with anti-human CD99 (Serotech clone O13), anti-human Ki67 (DAKO M7240), anti-human Fli-1 (BD PharMingen, 554266), anti-mouse CD31 (NeoMarkers), and anti-human CD31 (DAKO) antibodies. Horseradish peroxidase staining was performed using biotin-conjugated horse anti-mouse or goat anti-rabbit immunoglobulins (Vector Laboratories) and revealed with a DAKO 3,3′-diaminobenzidine kit (DAKO). For cell culture staining, cells were fixed for 20 min at room temperature with 4% paraformaldehyde and then subjected to Oil-Red-O and Von Kossa staining according to standard protocols. Pellets of ESFT cancer stem cells (ET-CSC) that had differentiated along the chondrogenic lineage were frozen in optimal cutting temperature compound (Tissue-Tek), cut into 5-μm-thick sections and stained with anti-collagen type II antibody (clone II-II6B3 mouse IgG_1, 1:2 dilution; Developmental Studies Hybridoma Bank, University of Iowa, IO) as described (14).

Real-time quantitative reverse transcription-PCR. cDNA was obtained using Moloney murine leukemia virus reverse transcriptase and RNase H minus (Promega). Typically, 250 ng of template total RNA and 250 ng of random hexamers were used per reaction. Real-time PCR amplification was performed using a TaqMan Universal PCR mastermix and Assays-On-Demand gene expression products or Power SYBR mix and specific PCR primers in an ABI Prism 7900 instrument (Applied Biosystems). Relative quantification of each target, normalized to an endogenous control (cyclophyllin A), was performed using a comparative Ct method (Applied Biosystems). Probes used included human POU5F1 (Hs 01895061_u1), NANOG (Hs02387400_g1), SOX2 (Hs00602736_s1), and MYC (Hs00153408_m1; Assays-On-Demand gene expression; Applied Biosystems). SYBR Green gene expression analysis for EWS-FLI-1 was achieved using published primer sequences (15).

Results and Discussion

To assess the presence of putative ET-CSC, surgical samples of ESFT, freshly removed from three patients (Supplemental Data 1A), were subjected to mechanical and enzymatic disaggregation. The resulting cell suspensions were tested for the presence of cells expressing CD133, a phylogenetically conserved cell surface molecule that has been associated with CSCs in glioblastomas (8), colon (13), and pancreatic (12) carcinomas. FACS analysis revealed that 4% to 8% of bulk ESFT cell populations expressed CD133 (Fig. 1*A*; Supplemental Data 1A). Immunohistochemical analysis of additional frozen tumor samples confirmed the presence of rare CD133+ tumor cells in five of five samples tested (Fig. 1*B*; Supplemental Data 1A). CD133+ and CD133− populations were therefore purified using CD133 magnetic bead cell sorting and their respective *in vivo* tumor-initiating potential was tested by injecting both cellular fractions in replicate serial dilutions into the subcapsular renal compartment of sublethally irradiated NOD/SCID mice. Examination of the kidneys 12 to 16 weeks following injection revealed that as few as 2,500 CD133+ cells were sufficient to initiate tumor formation in a fraction of injected mice, and that 10,000 CD133+ cells formed tumors in nearly all injected animals (Table 1). Injection of 50,000 CD133+ resulted in massive tumor formation in all animals (Fig. 2*A*). By contrast, injection of 50,000 CD133− cells failed to display any tumor-forming capacity *in vivo* (zero of six mice developed tumors with 2,500, 10,000, or 50,000 injected CD133− cells; Table 1; Fig. 2*B*). To determine whether CD133− cells were still detectable at the injection sites, we performed immunohistochemical analysis on paraffin-embedded

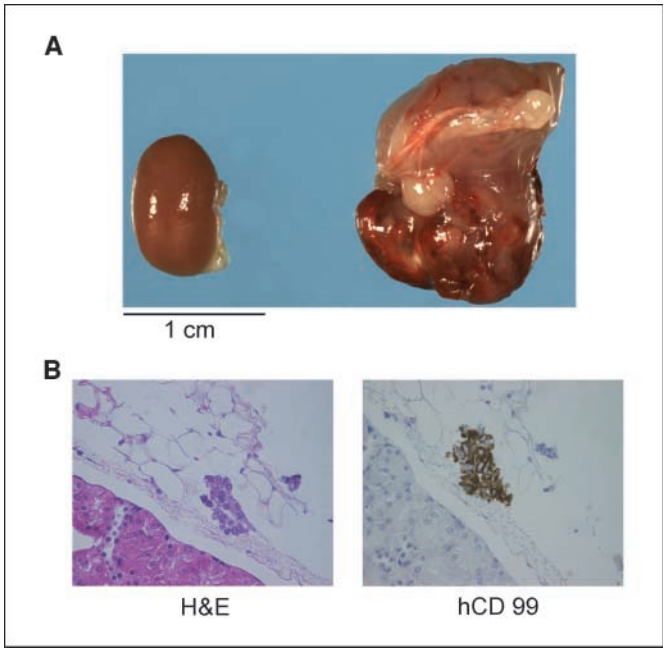

Figure 2. CD133+ but not CD133− cells form tumors in NOD/SCID mice. *A,* macroscopic image of a tumor derived from 50,000 CD133+ cells, 4 mo after injection beneath the renal capsule. The contralateral healthy kidney and scale are shown. *B,* H&E staining and anti-hCD99 immunohistochemical analysis of paraffin-embedded sections of a kidney, 4 mo after injection of 50,000 CD133− cells, showing the presence of viable CD99+ cells but no tumor formation. Magnification, ×200.

sections of kidneys that had been injected with 50,000 CD133− cells using an anti-human anti-CD99 antibody (CD99 being among the most reliable cell surface markers of ESFT). Small clusters of viable CD99+ cells were detected under the renal capsule, indicating that despite being able to engraft, these cells could not initiate tumor growth in NOD/SCID mice (Fig. 2*B*) as late as 4 months after injection.

To provide further evidence that the highly tumorigenic CD133+ fraction represents a CSC population, we performed serial transplantation assays of CD133+ and CD133− cells derived from primary xenografts, selecting one tumor from each patient (ESFT 1–3) for further transplantation into six recipient mice. Consistent with *in vivo* self-renewal properties ascribed to CSC, the CD133+ population displayed an unaltered ability to generate tumors in secondary and tertiary xenotransplantations (Table 1), whereas CD133− cells failed to form tumors (zero of six mice injected with 2,500, 10,000, and 50,000 CD133− cells in secondary and tertiary transplants). FACS analysis revealed that the percentage of CD133+ cells in all of the CD133+ cell-derived tumors, irrespective of passage number, was almost identical to that in the original tumor samples (Fig. 3*A*; data not shown), demonstrating that CD133+ ESFT cells have the ability to give rise to both CD133+ and CD133− cells, consistent with CSC properties. Histologic and immunohistochemical analysis showed that primary and secondary xenografts retained the phenotypic features of the parental tumors, characterized by sheets of CD99+ and FLI-1+ small round cells with scant stroma, and a comparable proliferation rate, as assessed by MIB-1 staining (Fig. 3*B*).

Because stromal cells play an important role in supporting and promoting tumor growth, an obvious concern related to the approach used to identify putative CSC from primary tumor

samples was the potential contribution to tumorigenesis by stromal elements present in the purified cell fractions. Endothelial cell precursors are typically CD133+ and may copurify with the CD133+ tumor cell fraction, possibly contributing to its ability to initiate tumor growth. We therefore assessed the origin of the endothelium in primary and secondary tumor transplants by immunohistochemistry using an anti-human CD31 antibody that does not cross-react with the corresponding mouse epitope. The vascular beds formed in all xenotransplants were composed exclusively of murine endothelial cells (Fig. 3*B, bottom*), indicating that human endothelial cell contamination could not explain the observed differences between CD133+ and CD133− tumor initiation potential in serial xenografts. An additional concern was that the CD133− cancer cell fraction may be diluted by CD133− stromal elements. Hence, we assessed *EWS-FLI-1* expression by quantitative real-time PCR in CD133+ and CD133− cell fractions, given that *EWS-FLI-1* is a marker of malignant cells only. The expression levels of *EWS-FLI-1* and of a selection of its established target genes (3, 16–20) were almost identical in the two cell fractions, irrespective of the passage number (Fig. 4*C, right*; Supplemental Data 1B), confirming that they contain a similar proportion of cancer cells.

Together, these observations provide experimental support to the notion that ESFT development does not occur according to the

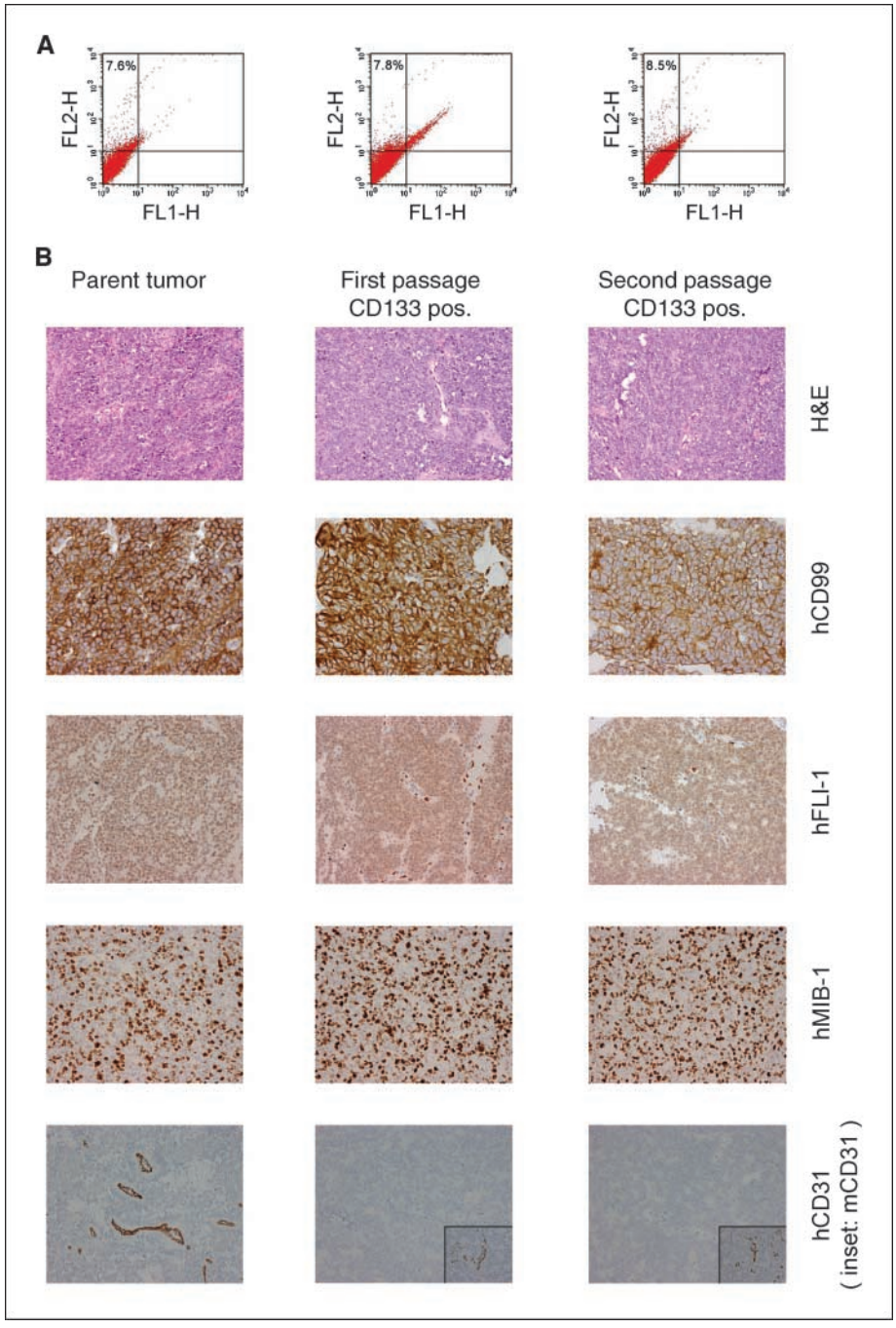

Figure 3. Tumor xenografts generated by serial injection of CD133+ cells display a similar CD133+ fraction and an identical histologic phenotype to those of the parental tumor. *A,* CD133 phycoerythrin FACS analysis of a single cell suspension derived from a parental ESFT (*left*), and the corresponding first and second passage CD133+ cell-derived tumor xenografts (*middle* and *right*, respectively), showing the preservation of a similar CD133+ population in all analyzed tumors. Experiments were performed at 12 wk after the injection of 50,000 CD133+ cells into the subcapsular renal compartment of NOD/SCID mice. *B,* histologic and immunohistochemical assessment of the same tumors as in *A*, showing that the serial xenografts share an identical small round cell morphology, a comparable staining pattern for the ESFTs markers CD99 and FLI-1, and a similar proliferation rate, as assessed by the MIB1 staining, with the parental tumor. *Bottom,* anti-human and anti-mouse CD31 staining, showing the exclusive mouse origin of endothelial cells in the serial xenotransplants (*insets*), in contrast to their human origin in the parental tumor. Magnification, ×100.

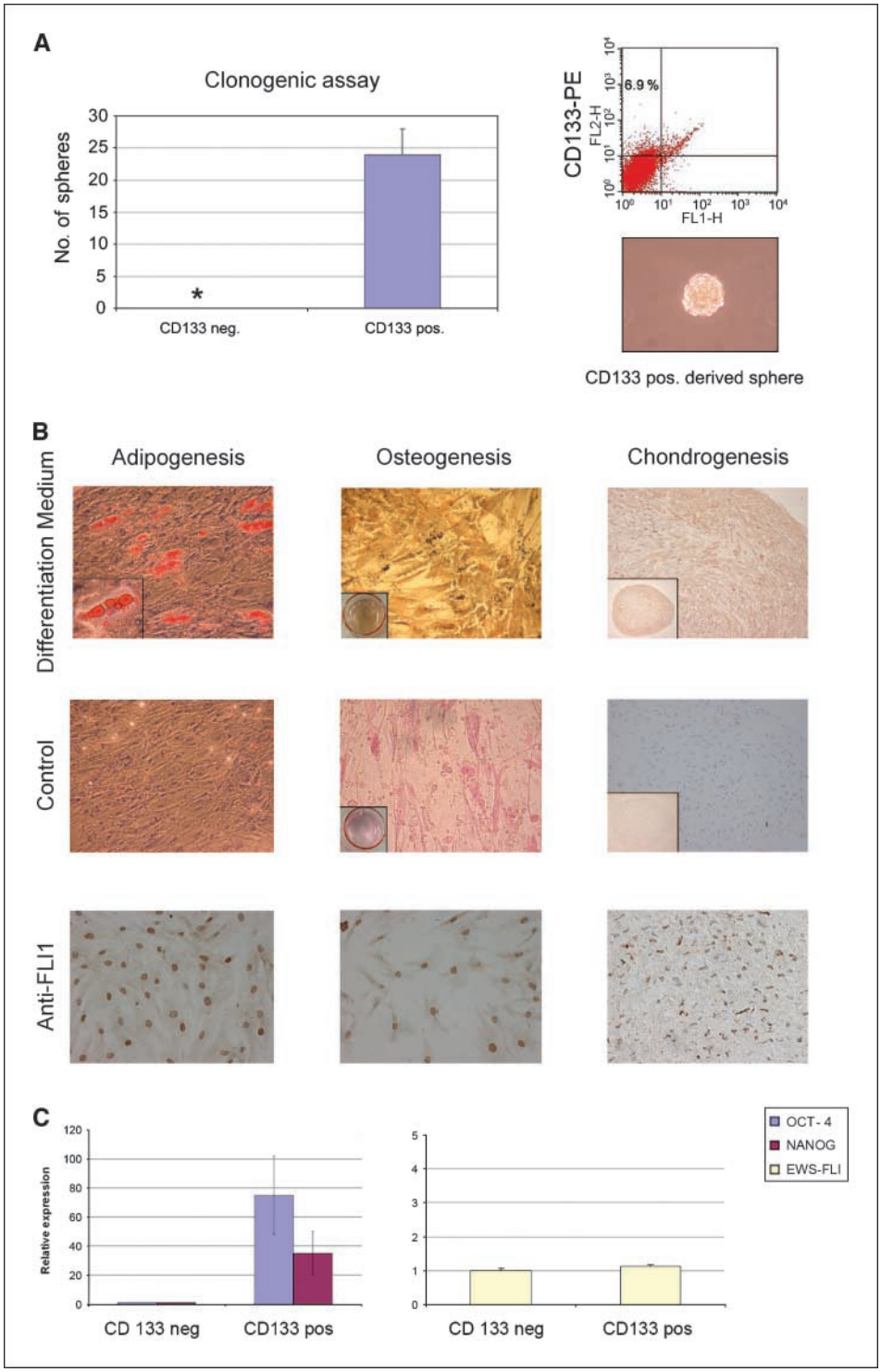

Figure 4. CD133+ cells display spherogenic potential, MSC plasticity, and high expression levels of the *OCT4* and *NANOG* genes. *A,* clonogenic assay (*left*). Single cells sorted for CD133 expression were plated in serum-free conditions, in 10 × 96 wells, and the total number of spheres was scored 30 d later (for further details, see Materials and Methods). The assay was performed in triplicate and the error bars indicate difference in the number of spheres formed in the three determinations. *, the CD133− fraction displayed a sphere formation frequency ranging from 0 to 1 sphere per 960 wells. *Right,* CD133 FACS analysis and photomicrograph of CD133+ cell–derived spheres. Magnification, ×400. *B,* differentiation assays of CD133+ cell–derived spheres show that they retain MSC plasticity (*top* and *middle*) and EWS-FLI-1 expression (*bottom,* anti-FLI-1 antibody). Spheres were briefly expanded as adherent cultures in MSC medium and then tested for MSC tri-lineage potential (for further details, see Materials and Methods). *Left,* adipocytic differentiation, Oil Red-O staining (*Control,* medium only); *center,* osteoblastic differentiation, Von Kossa staining (*Control,* medium only); *right,* chondrocytic differentiation, anti-collagen type II labeling counterstained with hematoxylin (*Control,* isotype-matched primary antibody). Magnifications, adipogenesis ×400 (*inset,* numerical magnification); osteogenesis ×400 (*inset,* image of the entire differentiation well); chondrogenesis ×200 (*inset,* ×40). *C,* real-time PCR analysis of *OCT4, NANOG* (*left*), and *EWS-FLI-1* (*right*) gene expression levels, in CD133+ and CD133− cell–derived RNA, showing that the CD133+ fraction expresses higher levels of *OCT4* and *NANOG* but a nearly identical level of the *EWS-FLI-1* fusion gene, suggesting an equal number of cancer cells in both fractions. The mean value observed in all samples tested is shown. All real-time PCR experiments were normalized to cyclophyllin A and done in triplicate. Error bars represent the variation between different samples measured in triplicate.

stochastic cancer model, in which each cancer cell has an equal tumor-initiating potential, but rather follows the CSC model, in which tumor initiation and sustained growth are governed by a defined tumor cell hierarchy.

Although no *in vitro* test is specific for CSC, some growth properties, such as spheroid formation in culture seems to be a potential CSC feature (21, 22). We therefore tested the ability of freshly isolated CD133+ and CD133− cells to form spheres in serum-free culture conditions. Because of the high sensitivity of this assay to potential CD133+ contaminant cells in the negative fraction, we performed a second round of depletion on the CD133− fraction (see Materials and Methods for details). Purified single cell suspensions were seeded in triplicate onto 960 wells and cellular spheres were scored 30 days later. The CD133+ fraction was found to display spherogenic capacity in serum-free conditions, whereas no sphere formation was observed in the CD133− fraction (Fig. 4*A, left*). Similarly, the shorter-term *in vitro* growth curve of CD133+ and CD133− cells in serum-free conditions showed a higher

proliferation rate of CD133+ cells (Supplemental Data 1C). We then tested CD133+ derived spheres by FACS analysis to determine the percentage of CD133+ cells present and found it to be similar to that in the parental tumors and xenografts (Fig. 4*A, right*). Serum-free–grown cellular spheroids thus allow *in vitro* propagation of ET-CSC.

If ESFT arise as a result of transformation of stem or progenitor cells, they may be expected to conserve some of the properties of their cell of origin. Recent work from our own (3, 4), as well as other laboratories (5), has raised the possibility that ESFTs originate from primary MSCs. We therefore addressed the possibility that ET-CSC might conserve some degree of MSC plasticity by assessing their capacity to differentiate into three major mesenchymal lineages, i.e., adipocytes, osteocytes, and chondrocytes. CD133 positive-derived spheres were briefly expanded in MSC medium, and subsequently cultured under the appropriate differentiation or control conditions, according to a protocol previously used to induce differentiation of primary MSCs (14). Surprisingly, ET-CSCs were observed to differentiate along all three lineages, as illustrated by Oil-Red-O (adipogenesis), Von Kossa (osteogenesis), and anti-collagen II antibody (chondrogenesis) staining (Fig. 4*B*). Thus, unlike ESFT cell lines that require silencing of EWS-FLI-1 to partially differentiate into mesenchymal lineages (5), primary ET-CSC retain a marked tri-lineage MSC plasticity in spite of EWS-FLI-1 expression (Fig. 4*B, bottom*). These observations are consistent with our recent data showing that introduction of the *EWS-FLI-1* fusion gene into primary MSCs does not alter their plasticity (4). Similar to leukemias and glioblastomas (22), sarcoma-initiating cells may therefore conserve the properties of their physiologic precursors.

The capacity for self-renewal and the maintenance of MSC plasticity would predict that CD133+ cells express genes implicated in stem cell maintenance. We therefore assessed, by quantitative real-time PCR, the expression of genes that play a prominent role in stem cell maintenance and nuclear reprogramming, including *MYC, SOX2, OCT4*, and *NANOG* (23–25), in the CD133+ and CD133− cell populations. *OCT4* and *NANOG* expression levels were consistently and significantly higher in the CD133+ fraction from all of the samples and cell isolates tested (Fig. 4*C, left*; data not shown). By contrast, *MYC* and *SOX2*, both of which are EWS-FLI-1 target genes (4), were comparably expressed in the two populations (data not shown), consistent with the equal expression level of the *EWS-FLI-1* fusion gene (ref. 15; Fig. 4*C, right*). Importantly, differences in *OCT4* and *NANOG* expression levels between primary CD133+ and CD133− cancer cell populations support the notion that the observed cellular hierarchy is based on intrinsic cellular properties and is not merely a reflection of the xenograft model used.

Isolation of a CD133+ cancer cell subpopulation in ESFT that displays tumor-initiating and *in vivo* self-renewing properties provides new insight into the biology of these tumors and constitutes the first identification of CSCs in a human sarcoma. The differentiation potential of ET-CSC strongly suggests that they represent transformed MSCs, further supporting an MSC origin for ESFT. Finally, due to their ability to reconstitute the original tumor phenotype and cellular hierarchy, ET-CSC represents the driving force that sustains tumor growth, and may therefore provide a valuable target for the design of therapeutic strategies aimed toward improving ESFT prognosis.

Disclosure of Potential Conflicts of Interest

The authors declare that they have no competing financial interests.

Acknowledgments

Received 6/13/2008; revised 12/3/2008; accepted 12/5/2008; published OnlineFirst 02/10/2009.

Grant support: FNRS grant 3100A0-105833, OCS grant 01656-02-2005, and a grant from the NCCR Molecular Oncology (I. Stamenkovic).

The costs of publication of this article were defrayed in part by the payment of page charges. This article must therefore be hereby marked *advertisement* in accordance with 18 U.S.C. Section 1734 solely to indicate this fact.

We thank Pierre Hoffmeyer and Vincent Kindler for fruitful collaboration, and Carlo Fusco, Laetitia Mauti, and Phil Shaw for insightful discussions.

References

1. Delattre O, Zucman J, Plougastel B, et al. Gene fusion with an ETS DNA-binding domain caused by chromosome translocation in human tumours. Nature 1992;359:162–5.
2. Riggi N, Cironi L, Suva ML, Stamenkovic I. Sarcomas: genetics, signalling, and cellular origins. Part 1: The fellowship of TET. J Pathol 2007;213:4–20.
3. Riggi N, Cironi L, Provero P, et al. Development of Ewing's sarcoma from primary bone marrow-derived mesenchymal progenitor cells. Cancer Res 2005;65:11459–68.
4. Riggi N, Suva ML, Suva D, et al. EWS-FLI-1 expression triggers a Ewing's sarcoma initiation program in primary human mesenchymal stem cells. Cancer Res 2008;68:2176–85.
5. Tirode F, Laud-Duval K, Prieur A, Delorme B, Charbord P, Delattre O. Mesenchymal stem cell features of Ewing tumors. Cancer Cell 2007;11:421–9.
6. Clarke MF, Dick JE, Dirks PB, et al. Cancer stem cells—perspectives on current status and future directions: AACR Workshop on Cancer Stem Cells. Cancer Res 2006;66:9339–44.
7. Lapidot T, Sirard C, Vormoor J, et al. A cell initiating human acute myeloid leukaemia after transplantation into SCID mice. Nature 1994;367:645–8.
8. Singh SK, Hawkins C, Clarke ID, et al. Identification of human brain tumour initiating cells. Nature 2004;432:396–401.
9. Galli R, Binda E, Orfanelli U, et al. Isolation and characterization of tumorigenic, stem-like neural precursors from human glioblastoma. Cancer Res 2004;64:7011–21.
10. Schatton T, Murphy GF, Frank NY, et al. Identification of cells initiating human melanomas. Nature 2008;451:345–9.
11. Al-Hajj M, Wicha MS, Benito-Hernandez A, Morrison SJ, Clarke MF. Prospective identification of tumorigenic breast cancer cells. Proc Natl Acad Sci U S A 2003;100:3983–8.
12. Hermann PC, Huber SL, Herrler T, et al. Distinct populations of cancer stem cells determine tumor growth and metastatic activity in human pancreatic cancer. Cell Stem Cell 2007;1:313–23.
13. O'Brien CA, Pollett A, Gallinger S, Dick JE. A human colon cancer cell capable of initiating tumour growth in immunodeficient mice. Nature 2007;445:106–10.
14. Suva D, Garavaglia G, Menetrey J, et al. Non-hematopoietic human bone marrow contains long-lasting, pluripotential mesenchymal stem cells. J Cell Physiol 2004;198:110–8.
15. Peter M, Gilbert E, Delattre O. A multiplex real-time PCR assay for the detection of gene fusions observed in solid tumors. Lab Invest 2001;81:905–12.
16. Kinsey M, Smith R, Lessnick SL. NR0B1 is required for the oncogenic phenotype mediated by EWS/FLI in Ewing's sarcoma. Mol Cancer Res 2006;4:851–9.
17. Prieur A, Tirode F, Cohen P, Delattre O. EWS/FLI-1 silencing and gene profiling of Ewing cells reveal downstream oncogenic pathways and a crucial role for repression of insulin-like growth factor binding protein 3. Mol Cell Biol 2004;24:7275–83.
18. Wai DH, Schaefer KL, Schramm A, et al. Expression analysis of pediatric solid tumor cell lines using oligonucleotide microarrays. Int J Oncol 2002;20:441–51.
19. Tirado OM, Mateo-Lozano S, Villar J, et al. Caveolin-1 (CAV1) is a target of EWS/FLI-1 and a key determinant of the oncogenic phenotype and tumorigenicity of Ewing's sarcoma cells. Cancer Res 2006;66:9937–47.
20. Cironi L, Riggi N, Provero P, et al. IGF1 is a common target gene of Ewing's sarcoma fusion proteins in mesenchymal progenitor cells. PLoS ONE 2008;3:e2634.
21. Todaro M, Alea MP, Di Stefano AB, et al. Colon cancer stem cells dictate tumor growth and resist cell death by production of interleukin-4. Cell Stem Cell 2007;1:389–402.
22. Singh SK, Clarke ID, Terasaki M, et al. Identification of a cancer stem cell in human brain tumors. Cancer Res 2003;63:5821–8.
23. Okita K, Ichisaka T, Yamanaka S. Generation of germline-competent induced pluripotent stem cells. Nature 2007;448:313–7.
24. Takahashi K, Yamanaka S. Induction of pluripotent stem cells from mouse embryonic and adult fibroblast cultures by defined factors. Cell 2006;126:663–76.
25. Wernig M, Meissner A, Foreman R, et al. *In vitro* reprogramming of fibroblasts into a pluripotent ES-cell-like state. Nature 2007;448:318–24.